

BASIC—ALIMENTARY TRACT

ATG16L1 and NOD2 Interact in an Autophagy-Dependent Antibacterial Pathway Implicated in Crohn's Disease Pathogenesis

CRAIG R. HOMER,* AMY L. RICHMOND,* NANCY A. REBERT,*[‡] JEAN-PAUL ACHKAR,*[‡] and CHRISTINE MCDONALD*

*Department of Pathobiology, Lerner Research Institute, and [‡]Department of Gastroenterology and Hepatology, Digestive Disease Institute, Cleveland Clinic, Cleveland, Ohio

See editorial on page 1448.

BACKGROUND & AIMS: The identification of numerous genes that confer susceptibility to Crohn's disease (CD) indicates that this complex disease might arise from alterations in several genes with related functions. We examined the functional interaction between the CD risk genes *ATG16L1* and *NOD2* to identify an autophagy-dependent pathway that is altered by disease-associated variants. **METHODS:** We assessed Nod2 signaling and autophagy activation in response to muramyl dipeptide (MDP) by immunoblot, confocal microscopy, flow cytometry, reporter gene, and gentamicin protection assays in human epithelial cell lines and primary human macrophages and dendritic cells from healthy individuals. The requirement of Nod2 and *ATG16L1* expression and the effects of CD-associated variants in MDP-stimulated autophagy and Nod2-dependent signaling were assessed in cell lines manipulated by RNA interference, inhibitors, or *ATG16L1* or *NOD2* variants and in primary macrophages and dendritic cells from healthy genotyped donors. **RESULTS:** MDP stimulation of epithelial cells, macrophages, and dendritic cells activated autophagy and nuclear factor κ B and mitogen-activated protein kinase signaling; it also increased killing of *Salmonella*. These responses depended on *ATG16L1* and Nod2 expression and were impaired by CD-associated *NOD2* variants. Nod2-dependent signaling was not impaired in cells with the *ATG16L1* T300A genotype, which is associated with CD. However, the *ATG16L1* T300A variant blocked the increase in MDP-mediated killing of *Salmonella* only in epithelial cell lines and not primary macrophages or dendritic cells. **CONCLUSIONS: *ATG16L1* and *NOD2* are components of an autophagy-mediated antibacterial pathway that is altered in a cell- and function-specific manner by CD-associated mutations.**

Keywords: CARD15; Inflammatory Bowel Disease; Genetics; Mucosal Immunity.

Crohn's disease (CD) is a chronic and sometimes debilitating form of inflammatory bowel disease. The underlying cause of CD is unknown; however, it is clear that both environmental and genetic factors are required for its development. Substantial evidence implicates an altered immune response to microbial factors as an essential contributor to the pathogenesis of CD.¹ This is evidenced by studies showing that the chronic inflammation found in CD depends on the presence of the bacterial microflora and by clinical data of disease remission induced by fecal stream diversion or manipulation of the gut microflora.^{2,3}

Until recently, only one gene had been conclusively identified as a CD susceptibility gene, *NOD2*, which encodes an intracellular bacteria sensor of the Nod-like receptor (NLR) family.⁴ Nod2 senses the presence of muramyl dipeptide (MDP), a component of the peptidoglycan cell wall from both Gram-positive and Gram-negative bacteria. Nod2 activation results in proinflammatory and antibacterial molecule production dependent on cell signaling pathways mediated by RICK/RIP2, nuclear factor κ B (NF- κ B), and mitogen-activated protein kinases. Three major *NOD2* variants are associated with CD: 2 missense mutations, R702W and G908R, and 1 frameshift mutation, L1007fsinsC (L1007fs). Human studies suggest that these *NOD2* variants result in a loss of function.⁵

Recent genome-wide association studies have dramatically increased the number of CD-associated susceptibility genes.^{6–9} Two of these genes, *ATG16L1* and *IRGM*, modulate autophagy. Autophagy is a starvation-induced cell survival mechanism in which organelles are broken down and recycled to provide nutrients. This mechanism also plays crucial roles in the immune system for elimi-

Abbreviations used in this paper: GFP, green fluorescent protein; LC3, light chain 3; MDP, muramyl dipeptide; MFI, mean fluorescence intensity; NF- κ B, nuclear factor κ B; NLR, Nod-like receptor; RNAi, RNA interference; shRNA, short hairpin RNA; TLR, Toll-like receptor; TNF, tumor necrosis factor.

© 2010 by the AGA Institute
0016-5085/\$36.00

doi:10.1053/j.gastro.2010.07.006

nation of intracellular microbes, presentation of endogenous antigens via major histocompatibility complex class II, shaping B- and T-cell function, and defining central tolerance.¹⁰ Importantly, knockdown of *ATG16L1* or *IRGM* expression blocks autophagy and killing of intracellular pathogens such as *Salmonella typhimurium*, *Listeria monocytogenes*, *Mycobacterium tuberculosis*, *Toxoplasma gondii*, and adherent invasive *Escherichia coli*, some of which are associated with the pathogenesis of CD.¹¹ The only CD-associated *ATG16L1* variant, T300A, results in a specific defect in bacteria-induced autophagy.^{7,12} Therefore, defects in autophagy not only impact innate and adaptive immune responses to bacteria but are also implicated in the pathogenesis of CD.

In this study, we investigated whether *NOD2* and *ATG16L1* are components of a common antibacterial pathway that is disrupted by specific CD-associated mutations. Our data show that MDP stimulation activates autophagy as an antibacterial response and implicates autophagy in Nod2 activation by MDP. Our findings also suggest that CD-associated variants of *NOD2* and *ATG16L1* result in defects in an autophagy-dependent antibacterial pathway specifically in epithelial cells.

Materials and Methods

Reagents

MDP and MDP-LL were purchased from Bachem (Torrance, CA), 3-methyl adenine and chloroquine from Sigma (St Louis, MO), lipopolysaccharide from InvivoGen (San Diego, CA), and rapamycin from LC Laboratories (Woburn, MA). Cytokines were obtained from Peprotech Inc (Rocky Hill, NJ).

Cell Lines

HEK293T and HCT116 (gifts of Gabriel Nuñez, University of Michigan, Ann Arbor, MI) as well as HT29GR cells (gift of Gerhard Rogler, University of Zurich, Zurich, Switzerland) were maintained in Dulbecco's Modified Eagle Medium (Invitrogen, Carlsbad, CA) with 10% fetal bovine serum (Lonza, Allendale, NJ) and penicillin/streptomycin (Invitrogen). HCT116 cells stably expressing EGFP-LC3 (HCT116:LC3) were created by transfection with PolyFect (Qiagen, Valencia, CA), G418 selection (Invitrogen), and then fluorescence-activated cell sorting to select low-expressing clones. HT29 cells (gift of Carol de la Motte, Cleveland Clinic, Cleveland, OH) were maintained in RPMI 1640 (Invitrogen) with 10% fetal bovine serum and penicillin/streptomycin. Cells were transfected by PolyFect or Amaxa nucleofection (Lonza) according to the manufacturer's instructions.

Primary Cells

Peripheral blood-derived mononuclear cells were obtained from healthy donors using protocols approved by the Cleveland Clinic Institutional Review Board.

Monocytes were obtained by counterflow centrifugal elutriation by the Cleveland Clinic Clinical and Translational Sciences Collaborative or purified from venous blood by Histopaque-1077 density gradient (Sigma) followed by negative selection using EasySep Monocyte Enrichment Kit Without CD16 Depletion (Stem Cell Technologies, Vancouver, British Columbia, Canada). Monocytes were differentiated over 6 to 7 days through the addition of cytokines into dendritic cells (100 ng/mL interleukin-4, 80 ng/mL granulocyte-macrophage colony-stimulating factor) or macrophages (50 ng/mL macrophage colony-stimulating factor). Donors were screened for *NOD2* and *ATG16L1* CD-associated variants by TaqMan SNP genotyping (Applied Biosystems, Foster City, CA) or restriction fragment length polymorphism analysis.

Plasmids and RNA Interference

NLR plasmids have been previously described.¹³ Dominant negative IKK constructs were gifts of Derek Abbott (Case Western Reserve University, Cleveland, OH). EGFP-tagged LC3 and kinase-dead Vps34 plasmids were obtained from Tony Eissa (Baylor University, Waco, TX), myc-ATG16L1 was from Origene Technologies Inc (Rockville, MD), and *NOD2* (NM_022162.1-2959s1c1), *ATG16L1* (NM_030803.5-2181s1c1), and nonspecific control (SHC002) MISSION small hairpin RNAs (shRNA) were purchased from Sigma. Beclin-1 shRNA and its matching control were gifts of William Maltese (University of Toledo, Toledo, OH). RICK shRNA (V2HS_17019) and pSmc2 were obtained from Open Biosystems (Huntsville, AL).

Immunoblots

Immunoblots were performed on whole cell lysates with antibodies to LC3 (Novus Biologicals, Littleton, CO), tubulin (Sigma), *ATG16L1* (Abgent, San Diego, CA), Beclin-1 (Novus Biologicals), green fluorescent protein (GFP; Santa Cruz Biotechnology Inc, Santa Cruz, CA), HA (Covance Research Products, Princeton, NJ), phosphorylated I κ B α , phosphorylated p38, or glyceraldehyde-3-phosphate dehydrogenase (Cell Signaling Technology, Boston, MA).

Luciferase Reporter Assays

Assays were performed as previously described.¹³ Cells were transfected in triplicate with NF- κ B luciferase reporter, β -galactosidase transfection control construct, and expression plasmids. Cells were stimulated with ligands for 16 hours and lysates assayed using the Luciferase Reporter Assay System (Promega, Madison, WI) and for β -galactosidase activity.¹³ Luciferase activity was normalized to β -galactosidase activity (nLuc).

Gentamicin Protection Assays

Intracellular killing of *Salmonella enterica* serovar *typhimurium* SL1344 (gift of Gabriel Nuñez) was assessed

by gentamicin protection assay.¹⁴ Overnight cultures in LB broth were incubated at 30°C, shaken at 180 rpm, and then diluted 1:7 and grown until $A_{600} = 0.5$. Cells were infected in triplicate at a multiplicity of infection of 10:1 for 30 minutes, washed with phosphate-buffered saline, and further incubated in gentamicin-supplemented Dulbecco's Modified Eagle Medium (50 $\mu\text{g}/\text{mL}$) for 1 hour (HEK293T, HCT116, macrophages, and dendritic cells) or 3 hours (HT29 and HT29GR cells). Cells were lysed in 1% Triton/phosphate-buffered saline for 10 minutes on ice and serial dilutions plated on LB agar in duplicate and grown overnight at 30°C. Colonies recovered were counted and colony-forming units per well calculated.

Flow Cytometry

HEK293T cells were plated at 10^5 cells/well and transfected with a total of 2 μg DNA (1 μg GFP-mCherry-LC3 [gift of Jaynatha Debnath, University of California, San Francisco]¹⁵ and 0.1 μg of NLR plasmids) using PolyFect according to the manufacturer's instructions. Forty-eight hours after transfection, cells were maintained in complete media and rapamycin treated (25 $\mu\text{g}/\text{mL}$ for 1 hour) or starved (Hanks' balanced salt solution for 2 hours), followed by collection in phosphate-buffered saline. A total of 10,000 live events were acquired on a FACSAria II multivariable cell sorter (Becton-Dickinson, San Jose, CA). Data were analyzed using FlowJo version 9.0.1 software (Tree Star, Ashland, OR). The target population was gated based on a forward-versus side-scatter plot, and transfected events were determined by GFP versus mCherry density plot. The mean fluorescence intensity (MFI) of each fluorochrome was determined in the target population. Results were expressed as GFP/mCherry MFI ratio normalized to untreated sample.

Cytokine Secretion Assay

Peripheral blood-derived mononuclear cells were plated in triplicate in RPMI plus 10% fetal bovine serum plus penicillin/streptomycin at 2×10^5 cells/well in 48-well plates and stimulated with 0, 0.1, or 1 $\mu\text{g}/\text{mL}$ MDP for 18 hours. Cell supernatants were assayed by Quantikine human TNF- α immunoassay (R&D Systems, Minneapolis, MN) according to the manufacturer's instructions.

Microscopy

HCT116:LC3 cells were MDP stimulated (10 $\mu\text{g}/\text{mL}$) or rapamycin stimulated (25 $\mu\text{g}/\text{mL}$), fixed in methanol, and mounted on slides using Vectashield plus DAPI (Vector Laboratories, Burlingame, CA). Samples were visualized by confocal microscopy using a 40 \times objective lens on a Leica TCS-SP spectral laser scanning confocal microscope equipped with a Q-Imaging Retiga EXi

cooled CCD camera and Image ProPlus Capture and Analysis software (Media Cybernetics, Silver Spring, MD). EGFP-LC3⁺ vesicles were scored in z-stack overlays from at least 4 separate fields. Autophagosome analysis was performed in an automated fashion using customized visual basic Image-Pro Plus macros. Transmission electron microscopy of HCT116:LC3 cells stimulated for 1 hour with MDP (10 $\mu\text{g}/\text{mL}$) was performed by the Cleveland Clinic Imaging Core Facility.

Statistical Analyses

Statistical significance between groups was determined by unpaired 2-tailed Student *t* test. For multiple group comparisons, data were analyzed by the Quantitative Health Sciences Department (Cleveland Clinic) using natural logarithm transformation to achieve normality, and results are summarized using mean and SD or confidence limits for the mean. Repeated-measures analysis of variance models were fit on the log-transformed responses, using *ATG16L1* genotype, MDP dose, and their interaction as predictors. An autoregressive correlation structure was used to model the association within each subject across MDP dose, as was a genotype-specific compound symmetry correlation structure. Statistical analysis was performed using SAS software (version 9.1; SAS Institute Inc, Cary, NC). Differences were considered significant when $P < .05$.

Results

The Bacterial Cell Wall Component, Muramyl Dipeptide, Stimulates Autophagy

We examined the role of autophagy in Nod2-mediated responses in both dendritic and epithelial cells, both of which play significant roles in the pathogenesis of CD.¹ Specifically, we explored whether the Nod2 ligand MDP stimulates autophagy in primary human dendritic cells and the human colon epithelial cell line HCT116. The recruitment of microtubule-associated protein 1 light chain 3 (LC3) from the cytoplasm to vesicle membranes has been defined as a specific marker of autophagosomes.¹⁰ This process involves the modification of a soluble form of LC3 (LC3-I) to a lipidated form (LC3-II), which inserts into the forming autophagosomal membrane. This can be detected by a shift in molecular weight in an immunoblot or the localization of LC3 to vesicles by microscopy. We assessed autophagy induction by immunoblot and found that in both HCT116 and dendritic cells, MDP stimulation increased LC3-II levels within 30 minutes to 1 hour (Figure 1A and B). This result was confirmed by the microscopic examination of HCT116 cells stably expressing EGFP-LC3 (HCT116:LC3 cells), which showed a modest, but reproducible increase (~2-fold) in the number of LC3-positive cells after MDP stimulation (Figure 1C and D). Together, the results of

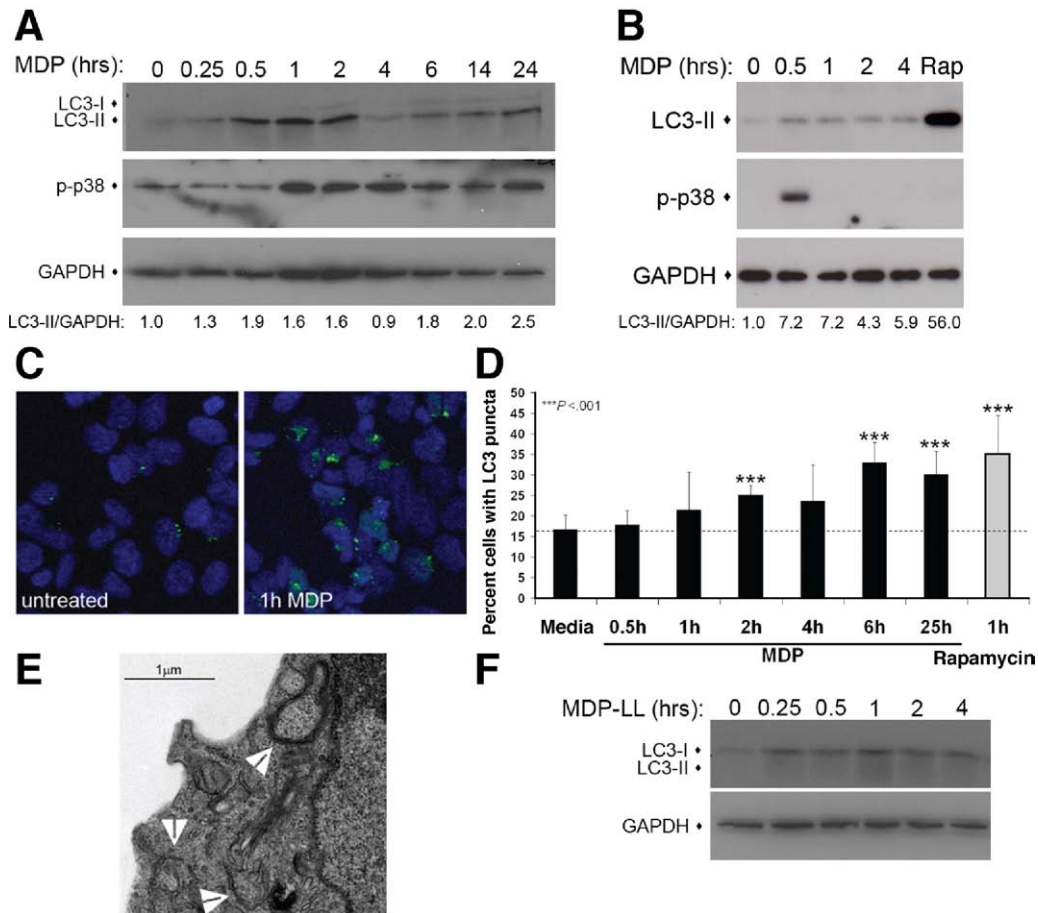


Figure 1. MDP stimulates autophagy in epithelial and dendritic cells. (A) Immunoblot of HCT116 cells treated with 10 $\mu\text{g}/\text{mL}$ MDP. LC3-II accumulation quantified by LC3-II/glyceraldehyde-3-phosphate dehydrogenase ratio. p-p38, phosphorylated p38. (B) Assay performed as in A with primary human dendritic cells. (C) Confocal micrographs of HCT116 expressing EGFP-LC3 (green) in media or MDP-stimulated (20 $\mu\text{g}/\text{mL}$) for 1 hour. (D) Quantification of cells with punctuate EGFP-LC3 (mean \pm SD), $n \geq 4$ fields with >50 cells/field. (E) Electron micrograph of MDP-stimulated HCT116:LC3 cells (10 $\mu\text{g}/\text{mL}$ for 1 hour). Arrows indicate autophagosomes. (F) Immunoblot of MDP-LL-stimulated (10 $\mu\text{g}/\text{mL}$) HCT116 cells.

these 2 assays show LC3-II accumulation preceding the formation of LC3-positive puncta. The formation of autophagosomes was further confirmed by electron microscopy in MDP-stimulated HCT116:LC3 cells (Figure 1E). This increase in autophagy was specific to the stimulatory form of MDP, because treatment of HCT116 cells with a nonstimulatory MDP isomer, MDP-LL, did not increase LC3-II levels (Figure 1F).

We assessed the effect of MDP stimulation on the killing of an intracellular pathogen, *Salmonella typhimurium*, to measure autophagy in the context of an immune response. *Salmonella* is targeted by autophagy and has become a model organism to study the autophagic process.¹⁶ We confirmed that *Salmonella* infection induces an autophagic response by increasing LC3-II accumulation in immunoblots of HCT116 cell lysates (Supplementary Figure 1A). In addition, rapamycin stimulation of autophagy increased *Salmonella* killing in gentamicin protection assays, while reduction of ATG16L1 expression by RNA interference (RNAi) decreased bacterial clearance (Supplementary Figure 1B and C and Supplementary

Figure 2D). Using this system, we asked whether MDP-stimulated autophagy enhanced the clearance of intracellular *Salmonella* infection. MDP stimulation of HCT116 cells during infection significantly increased *Salmonella* killing (Figure 2A). This antibacterial effect was specific to the stimulatory form of MDP, because treatment with MDP-LL had no effect. The MDP enhancement of bacterial killing was autophagy dependent, because RNAi knockdown of ATG16L1 expression abrogated the MDP response (Figure 2B). Similar results were observed in both primary human macrophages and dendritic cells infected with *Salmonella* (Figure 2C). These results show that MDP stimulation of autophagy results in increased antibacterial activity in both primary immune cells and epithelial cells.

Nod2 Is Necessary and Sufficient for Muramyl Dipeptide-Stimulated Autophagic Responses

With the generation of Nod2-deficient mice, it has been shown that Nod2 mediates most of the cel-

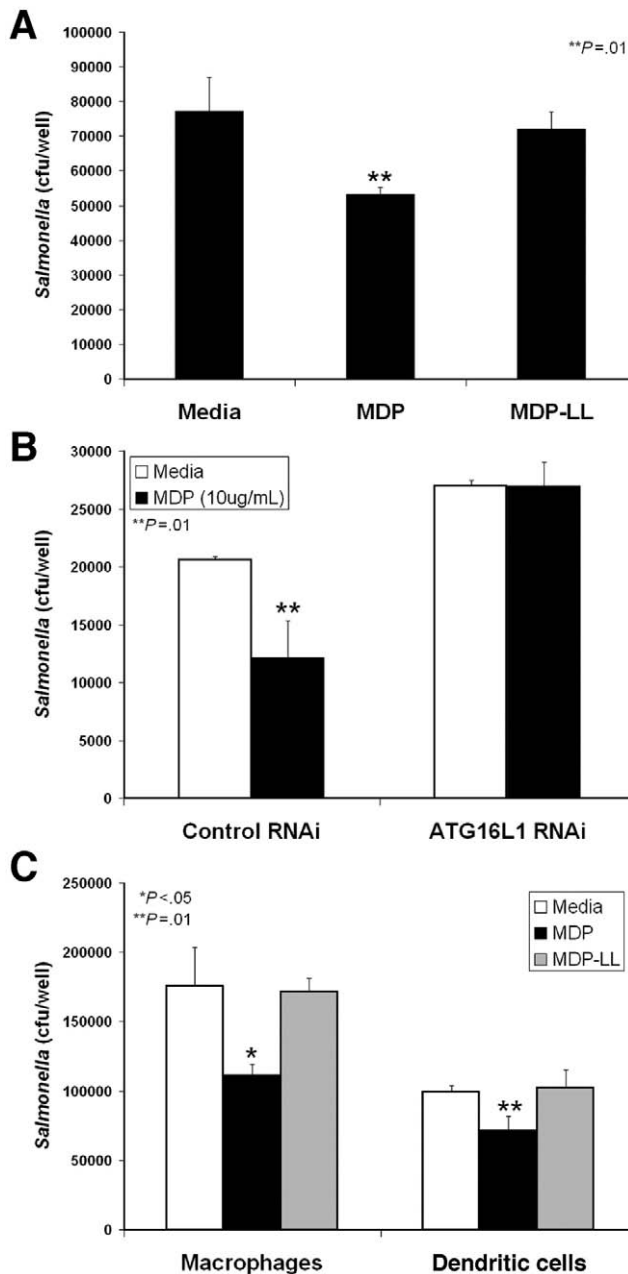


Figure 2. MDP enhances *Salmonella* killing via an *ATG16L1*-dependent mechanism in gentamicin protection assays. (A) Infected HCT116 cells treated with media, MDP (10 µg/mL), or MDP-LL (10 µg/mL) (mean ± SD). (B) HCT116 cells transfected with control or *ATG16L1* RNAi constructs and infected with or without MDP (10 µg/mL) (mean ± SD). (C) Assay performed as in A using primary human macrophages or dendritic cells (mean ± SD).

lular effects of MDP.¹⁷ However, additional NLRs are activated by MDP, such as NLRP3, to activate caspase-1 and cause secretion of interleukin-1β and interleukin-18.¹⁸ Therefore, we investigated the requirement of Nod2 in autophagic antibacterial killing in response to MDP stimulation. We found MDP-enhanced *Salmonella* killing was blocked in HCT116 cells transfected with Nod2 RNAi (Figure 3A), indicat-

ing that Nod2 expression is required for MDP-enhanced antibacterial activity.

Next, we investigated whether Nod2 activity is sufficient for an antibacterial response mediated by autophagy. For these experiments, we used HEK293T cells transiently transfected with NLR expression constructs. HEK293T cells do not express detectable levels of NLR or Toll-like receptor (TLR) proteins¹⁹ and therefore are commonly used to assess components of these microbial sensor pathways in isolation. In addition, NLR overexpression causes ligand-independent activation of these proteins.¹⁹ We found that Nod2 overexpression significantly increased *Salmonella* killing in a dose-dependent manner (Figure 3B). This Nod2-dependent increase was dependent on Nod2 signal transduction, because RNAi knockdown of the signaling adaptor RICK blocked Nod2-dependent antibacterial activity (Figure 3C). A similar increase was not observed when NLRP3 was expressed, suggesting that, of the NLRs activated by MDP, this effect is specific to Nod2 (Figure 3D). Autophagy is also required for this effect, because RNAi knockdown of *ATG16L1* expression decreased the basal level of *Salmonella* killing and blocked Nod2-enhanced killing (Figure 3D).

These findings were further confirmed as an autophagy-dependent response by a separate autophagy assay that detects the maturation of autophagosomes. The LC3-positive autophagosome matures through fusion with lysosomes, providing an acidic environment promoting degradation of autophagosome contents. Autophagosomal maturation can be tracked by a GFP-mCherry-LC3 tandem tagged construct, because the acidic environment in the mature autophagosome quenches the fluorescent signal of GFP but not the mCherry fluorophore.²⁰ Traditionally, the maturation of dual-positive autophagosomes to single mCherry-positive autophagosomes is quantified by fluorescent confocal microscopy. We adapted this method for analysis by flow cytometry to increase the speed of analysis and decrease investigator bias. In response to starvation or rapamycin treatment, HEK293T cells expressing GFP-mCherry-LC3 showed a significant decrease in GFP MFI without a similar change in mCherry fluorescence (Supplementary Figure 3C–F). This change is reflected in a statistically significant decreased GFP/mCherry ratio over a series of independent experiments (Supplementary Figure 3B). Using this system, we transfected HEK293T cells with GFP-mCherry-LC3 and vector, Nod2, or NLRP3 expression constructs and detected a significant increase in autophagosomal maturation in the Nod2-expressing population (Figure 3E). Expression of NLRP3 did not change the GFP/mCherry ratio (Figure 3E). These results show that MDP-stimulated antibacterial responses are mediated by Nod2 signaling and autophagy. In addition, Nod2 is sufficient to induce these effects when activated in a ligand-independent manner.

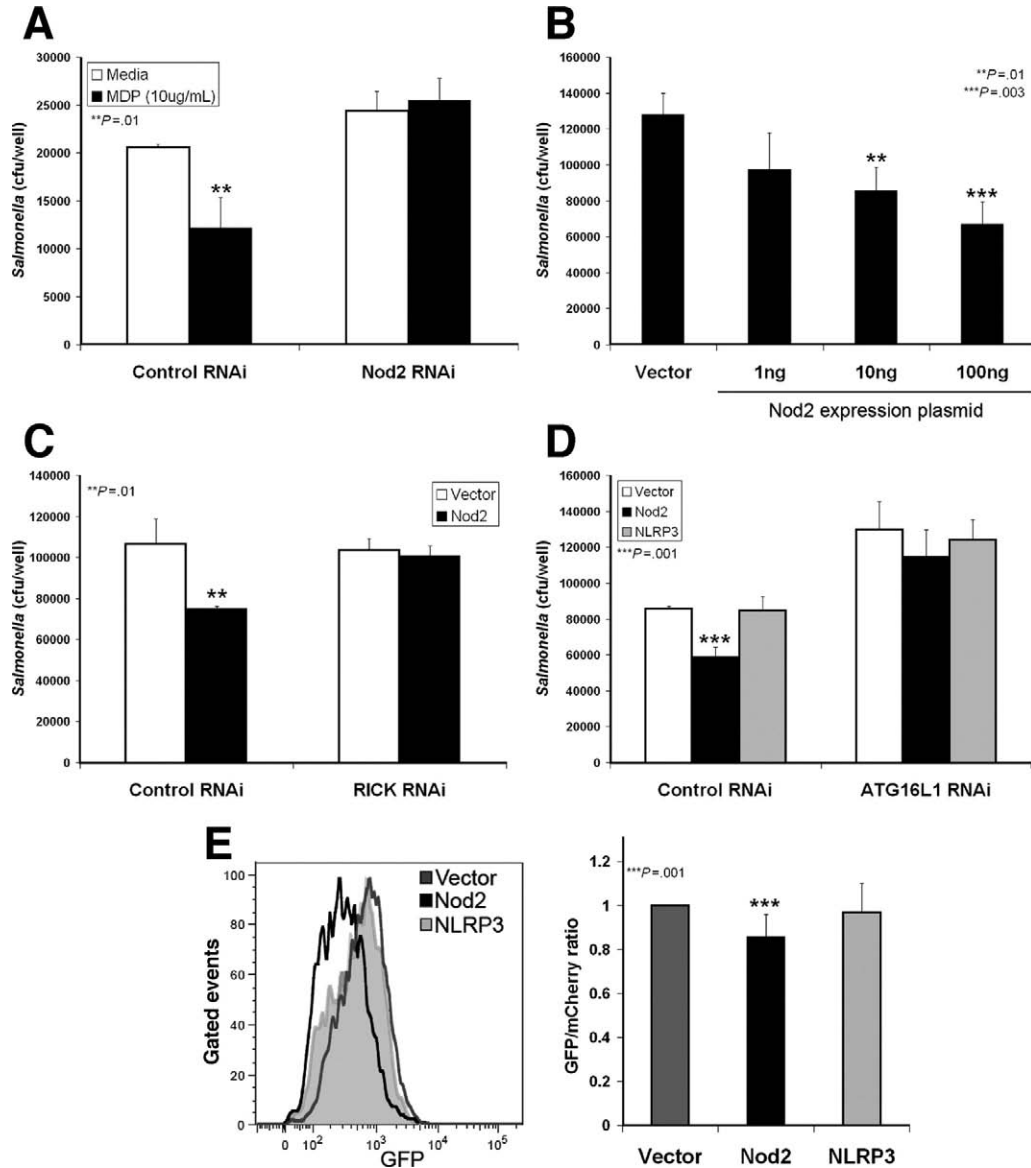


Figure 3. Nod2 is necessary and sufficient for MDP-enhanced *Salmonella* killing by autophagy. (A) HCT116 cells transfected with control or Nod2 RNAi and infected with or without MDP (10 μ g/mL) (mean \pm SD). (B) Gentamicin protection assay performed with HEK293T cells transfected with indicated amounts of Nod2 plasmid (mean \pm SD). (C) Control or RICK RNAi transfected HCT116 cells and infected with or without MDP (10 μ g/mL) (mean \pm SD). (D) Gentamicin protection assay performed with HEK293T cells transfected with vector, Nod2, or NLRP3 expression plasmid and control or ATG16L1 RNAi construct (mean \pm SD). (E) Autophagosomal maturation assessed by flow cytometric analysis of GFP-mCherry-LC3 in HEK293T cells transfected with vector, Nod2, or NLRP3 expression vectors. Histogram of GFP MFI of the mCherry-positive population (left). Quantification of GFP/mCherry MFI ratio normalized to vector transfected sample (mean \pm SD) (right, n = 4).

CD-Associated NOD2 Variants Are Impaired in Both Proinflammatory Signaling and Induction of Autophagy

Next, we assessed the activation of autophagic responses by CD-associated NOD2 variants. The responses of HEK293T cells transfected with expression plasmids for the 3 major CD-associated Nod2 variants were compared with cells transfected with wild-type Nod2 or empty vector. Consistent with previous reports,⁵ the Nod2 variants R702W and G908R activated significantly less NF- κ B activity than wild-type Nod2 in a lu-

ciferase reporter assay, while L1007fs was unable to activate the reporter (Figure 4A). When these Nod2 mutants were tested for enhancement of *Salmonella* killing, a similar profile was seen. The antibacterial killing by Nod2 was significantly impaired by the R702W and G908R mutations and completely lost by the L1007fs mutant (Figure 4B). A recent report described a role for the NF- κ B activating kinases IKK α and IKK β in activation of autophagy²¹; therefore, we investigated whether these IKKs are required for Nod2 enhancement of bacterial killing. Dominant negative IKK α and IKK β were ex-

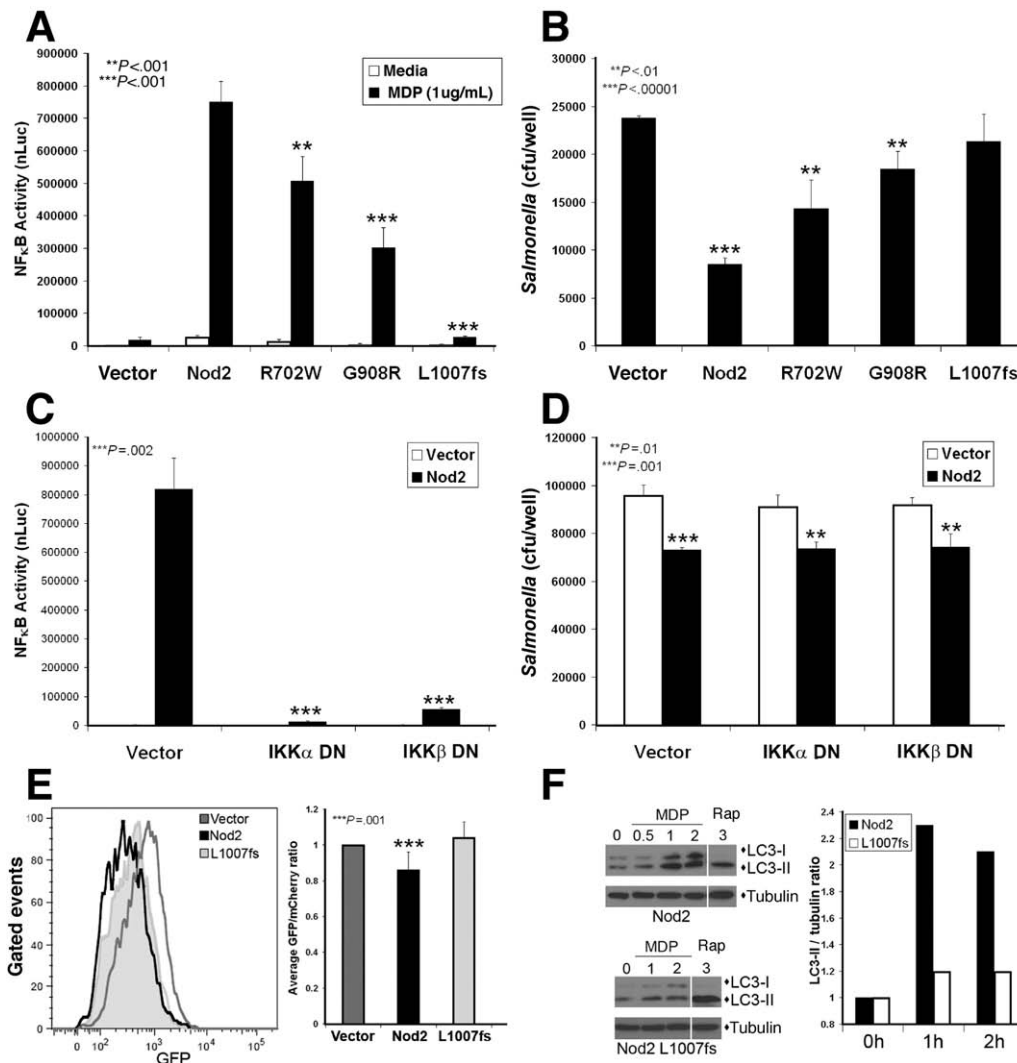


Figure 4. CD-associated *NOD2* mutants are impaired in signaling, antibacterial killing, and autophagy. (A) NF- κ B luciferase reporter assay in HEK293T cells transfected with *Nod2* plasmids and stimulated with MDP (1 μ g/mL) for 18 hours. Luciferase values normalized to β -gal transfection control (nLuc) (mean \pm SD). (B) Gentamicin protection assay of HEK293T cells transfected with *Nod2* plasmids (mean \pm SD). (C) NF- κ B luciferase reporter assay in HEK293T cells transfected with *Nod2* and IKK dominant negative (DN) constructs (mean \pm SD). (D) Gentamicin protection assay of HEK293T cells transfected with *Nod2* and IKK DN plasmids (mean \pm SD). (E) Autophagosomal maturation assessed by flow cytometric analysis of GFP-mCherry-LC3 in HEK293T cells transfected with vector, *Nod2*, or *Nod2* L1007fs plasmids. Histogram of GFP MFI of the mCherry-positive population (*left*). Quantification of GFP/mCherry MFI ratio normalized to vector transfected sample (mean \pm SD) (*right*, $n = 7$). (F) LC3 immunoblots of HEK293T cells transfected with *Nod2* or *Nod2* L1007fs plasmids treated with MDP (1 μ g/mL) or rapamycin (25 μ g/mL) for the indicated times (hours). Quantification of LC3-II amount indicated by LC3-II/tubulin ratio (*right*).

pressed in HEK293T cells to test their effect on *Nod2*-dependent functions. While both dominant negative IKKs blocked NF- κ B activity stimulated by *Nod2* overexpression (Figure 4C), *Nod2*-enhanced bacterial killing was unaffected (Figure 4D). These results indicate that CD-associated *Nod2* mutations decrease proinflammatory NF- κ B signaling as well as NF- κ B-independent antibacterial *Nod2* function.

Next, we examined whether the defect in *Salmonella* killing by CD-associated *Nod2* mutants is due to an impairment of autophagy. We assessed maturation of autophagosomes by 2 separate assays. Overexpression of *Nod2* in HEK293T cells, but not the L1007fs mutant,

induced autophagosome maturation, as reflected by a significant decrease in the GFP/mCherry ratio (Figure 4E). In addition, MDP-stimulated LC3-II accumulation in HEK293T cells transfected with low amounts of wild-type or L1007fs mutant *Nod2* was assessed by immunoblot. Significant changes in LC3-II levels were detected in cells expressing wild-type *Nod2* but not the L1007fs mutant (Figure 4F). This was not due to a global autophagy defect in these cells, because rapamycin treatment activated autophagy in both conditions. These results show that MDP-stimulated autophagy is a *Nod2*-dependent antibacterial response that may be altered in individuals carrying specific *NOD2* mutations.

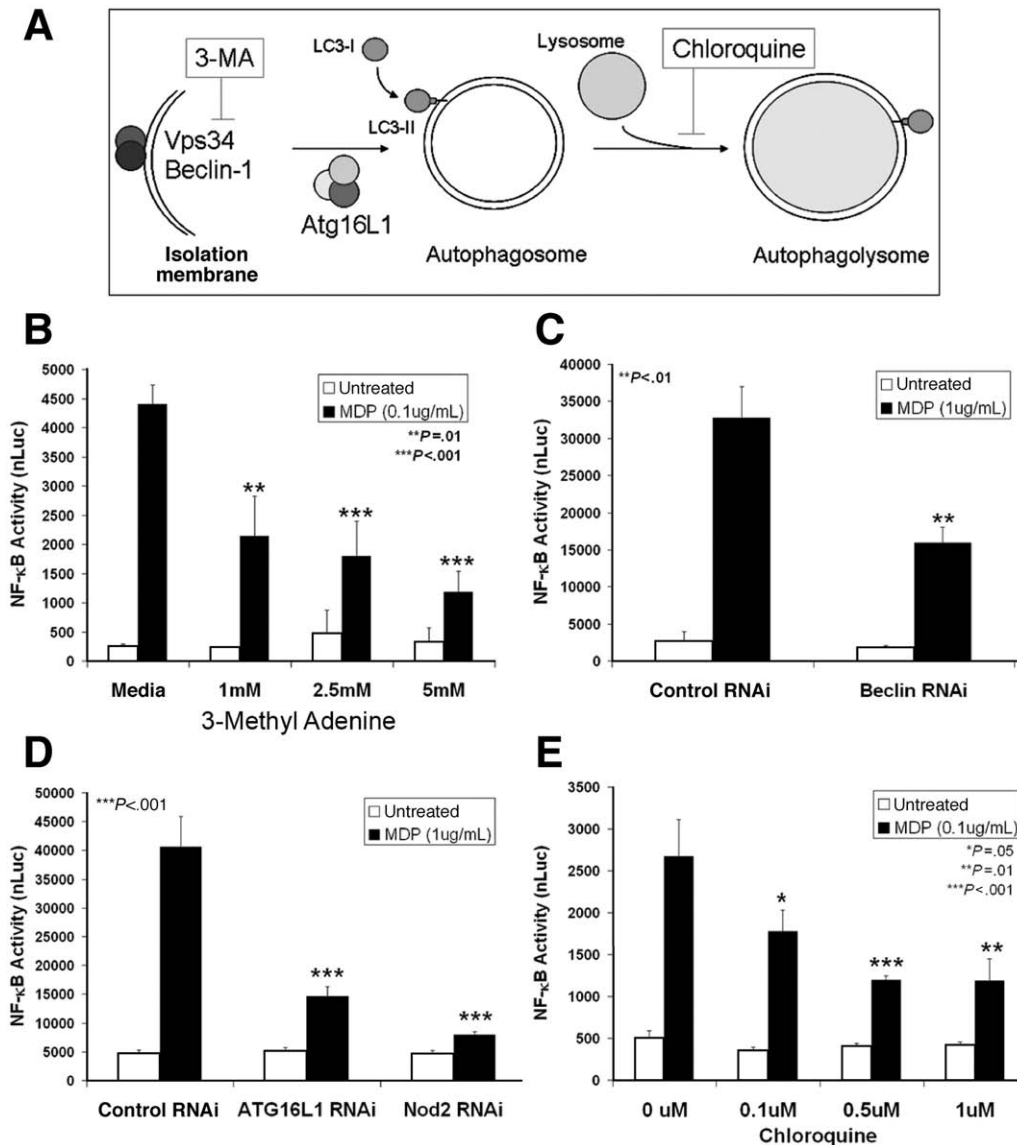


Figure 5. Inhibition of autophagy impairs activation of Nod2 signaling. NF- κ B luciferase reporter assays were performed in HCT116 cells in the presence of autophagy inhibitors. Luciferase values normalized to β -gal transfection control (nLuc) (mean \pm SD). (A) Steps of autophagosome formation and maturation with key molecules and action of inhibitors indicated. (B) Cells stimulated with MDP and indicated amounts of 3-methyl adenine. (C) Cells transfected with either control or Beclin-1 RNAi constructs. (D) Cells transfected with control, ATG16L1, or Nod2 RNAi constructs. (E) Cells stimulated with MDP and indicated amounts of chloroquine.

Inhibition of Autophagy Impairs Activation of Nod2 Signaling

MDP must be delivered to the cell cytosol to activate Nod2. MDP enters cells by a vesicular pathway and trafficks to an acidic compartment to stimulate Nod2 signaling.^{17,22,23} Many of the vesicular characteristics of MDP-containing vesicles are shared with autophagosomes, leading us to investigate whether autophagy is involved in the intracellular trafficking of MDP and activation of Nod2 signaling.

We tested the contribution of autophagy to Nod2 signaling activation using NF- κ B luciferase reporter assays in HCT116 cells. MDP activates both Nod2 and NLRP3; however, MDP stimulation of NF- κ B signaling is

a Nod2-dependent activity, as shown by previous studies¹⁷ and RNAi knockdown of Nod2 expression (Figure 5D). The first stage of autophagy is dependent on a phosphatidylinositol 3-kinase complex containing Vps34 and Beclin-1, which causes the formation of autophagic isolation membranes (Figure 5A). When initiation of autophagy was inhibited by treatment with a phosphatidylinositol 3-kinase inhibitor, 3-methyl adenine, or expression of a kinase-dead Vps34 mutant, Nod2 signaling was dose-dependently inhibited (Figure 5B and Supplementary Figure 4). Similarly, Nod2-dependent NF- κ B activation was decreased with RNAi knockdown of Beclin-1 expression (Figure 5C). ATG16L1 assists in the recruitment of LC3 to autophagosomal membranes mediating

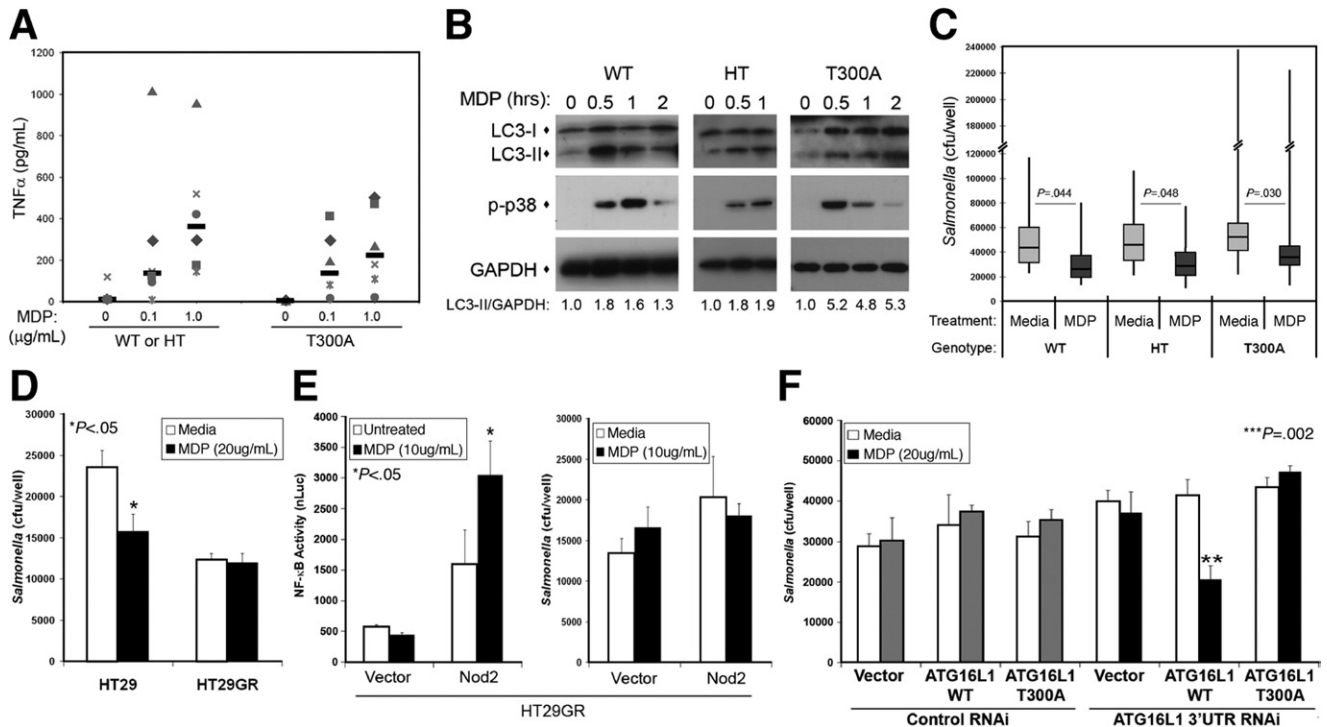


Figure 6. *ATG16L1* T300A impairs MDP-enhanced bacterial killing in a cell type-specific manner. (A) TNF- α secreted by MDP-stimulated peripheral blood-derived mononuclear cells (0, 0.1, or 1 $\mu\text{g}/\text{mL}$ for 18 hours) with the indicated genotypes; median values of the group ($n = 6$) are indicated by bars. WT, wild-type *ATG16L1*; HT, heterozygous *ATG16L1*; T300A, homozygous *ATG16L1* T300A. (B) Immunoblot analysis of MDP-stimulated, (10 $\mu\text{g}/\text{mL}$), genotyped dendritic cells. Induction of autophagy quantified by LC3-II accumulation indicated by LC3-II/glyceraldehyde-3-phosphate dehydrogenase ratio, with similar results seen by alternative quantification of LC3-I/LC3-II ratios. p-p38, phosphorylated p38. (C) Gentamicin protection assay of genotyped macrophages performed in media with or without MDP (10 $\mu\text{g}/\text{mL}$). Bars indicate the geometric mean values (WT, $n = 7$; HT, $n = 7$; T300A, $n = 14$) with the 95% confidence limits shown by the boxes. The range of response is indicated by the vertical bars. (D) Gentamicin protection assay of HT29 or HT29GR cells performed in media with or without MDP (20 $\mu\text{g}/\text{mL}$) (mean \pm SD). (E) NF- κB luciferase reporter assay (left) and gentamicin protection assay (right) in HT29GR cells transfected with vector or Nod2 plasmid and treated with MDP (10 $\mu\text{g}/\text{mL}$) (mean \pm SD). (F) Gentamicin protection assay of Nod2-expressing HT29GR cells transfected with vector, ATG16L1 or ATG16L1 T300A plasmids and control, or ATG16L1 RNAi performed in media with or without MDP (20 $\mu\text{g}/\text{mL}$) (mean \pm SD).

the elongation and closure of autophagosomes. RNAi-mediated knockdown of ATG16L1 impaired MDP-stimulated NF- κB signaling (Figure 5D). These findings show a novel, functional interaction between 2 CD risk genes whereby ATG16L1 expression affects Nod2 function. In addition, when lysosomal fusion was inhibited by chloroquine treatment, a dose-dependent reduction in Nod2 signaling was observed (Figure 5E). This result concurs with published data from mouse macrophages,²² in which bafilomycin A1 treatment inhibits Nod2 signaling. Our results show that inhibition of autophagy, at several distinct steps of the autophagy pathway, significantly decreases the activation of Nod2 signaling.

The CD-Associated ATG16L1 T300A Variant Specifically Impairs Nod2-Dependent Antibacterial Functions in Epithelial Cells

The CD-associated variant of *ATG16L1* T300A has specific reductions in bacteria-stimulated autophagy and not other forms of autophagy.^{12,24} Because loss of ATG16L1 expression had dramatic effects on Nod2 function, we examined whether the CD-associated variant of

ATG16L1 affected Nod2 function in both monocytic and epithelial cells.

We obtained monocytic cells from healthy donors genotyped for the *ATG16L1* T300A variant to test the effect of this variant on Nod2-dependent responses. First, we assessed activation of Nod2 signaling by measuring tumor necrosis factor (TNF)- α secretion (a cytokine central to the pathogenesis of CD and a target for CD therapy¹) and MDP-stimulated phosphorylation of signaling proteins. Studies suggest the T300A variant is a loss-of-function allele^{12,24}; therefore, we combined individuals heterozygous for the T300A variant and wild-type individuals and compared their responses with T300A homozygous individuals. We found no statistically significant differences in TNF- α secretion by MDP-stimulated peripheral blood-derived mononuclear cells in the 2 groups (Figure 6A). In addition, the timing and amplitude of Nod2 signaling in dendritic cells from these donors was not drastically different, as assessed by phosphorylation of p38 mitogen-activated protein kinase in immunoblots (Figure 6B). Autophagic responses were

not significantly altered either, because there were no consistent differences in the timing or amount of LC3-II accumulated in MDP-stimulated dendritic cells from wild-type, heterozygous, or homozygous donors (Figure 6B). Macrophages from all donor groups also had comparable mean basal *Salmonella* killing, and MDP-stimulated bacterial killing was increased by a similar amount (30%–40%; Figure 6C). These results suggest that the CD-associated *ATG16L1* T300A variant does not significantly affect Nod2 function in monocytic cells.

These findings are in contrast to the results obtained from epithelial cells. We tested Nod2 function in human colon epithelial cell lines screened for *ATG16L1* and *NOD2* risk alleles. We compared 2 different derivatives of the HT29 cell line, one of which has wild-type *ATG16L1* and expresses Nod2 (“HT29”) and the other of which has *ATG16L1* T300A and does not express Nod2 (“HT29GR”). Initially, we compared the MDP-induced functions of these cells. As expected, in the absence of Nod2 expression, MDP treatment of HT29GR cells did not enhance *Salmonella* killing (Figure 6D) or activation of an NF- κ B luciferase reporter (Figure 6E). When exogenous Nod2 is expressed by transfection in HT29GR cells, we saw a Nod2-dependent increase in basal NF- κ B luciferase reporter expression and an MDP-stimulated enhancement of its expression (Figure 6E). However, when Nod2-dependent antibacterial killing was measured in the same cells, we found no differences in the basal levels of *Salmonella* killing and no MDP-enhanced killing (Figure 6E). To determine if the *ATG16L1* T300A risk variant was responsible for this defect in bacterial killing, we knocked down expression of endogenous *ATG16L1* T300A using RNAi targeting the 3' untranslated region and expressed wild-type *ATG16L1* or mutant *ATG16L1* T300A in its place by transfection of complementary DNA expression plasmids. We saw a restoration of MDP-stimulated antibacterial killing in cells that now expressed wild-type *ATG16L1*, while expression of the mutant *ATG16L1* T300A was unable to complement the defect (Figure 6F). These results indicate that the CD-associated *ATG16L1* T300A risk variant causes a specific loss of Nod2 antibacterial function in colon epithelial cells.

Discussion

Great advances have been made in understanding the genetics of CD through the use of genome-wide association studies.^{6–9} However, significant challenges remain to identify the functional consequences of disease-associated variants and how they contribute to disease pathogenesis. Instead of focusing on the effects of a single gene, we examined the functional interplay of CD risk genes to identify common pathways altered by specific genetic variants. Although it is of great interest to study these pathways in the context of the disease, the inherent variability of patient-derived cells (ie, current inflammatory status, medications, disease subtype, and

so on) and limited amounts of sample make interpretation of results challenging in small sample sizes. Therefore, we examined the interplay of 2 CD risk genes in healthy individuals to reduce the complexity of our system and provide a basis for our future studies in patient-derived cells. Our findings show that *ATG16L1* and *NOD2* functionally interact in an autophagy-dependent antibacterial pathway that is altered by CD-associated variants in a cell type-specific manner.

Multiple links are evident between autophagy and microbial sensors. Autophagy has been shown to be activated by TLR signaling, playing a positive role in the control of mycobacteria.^{25–28} TLR-stimulated autophagy was shown to require signaling adaptor proteins, such as MyD88 and TRIF.^{25,27,28} Related studies proposed the requirement for a TLR-independent pathway in autophagic killing of *Salmonella*.²⁹ While our studies were under way, it was shown by 2 other groups that Nod2 activates autophagy to enhance intracellular bacterial killing.^{30,31} Cooney et al found that MDP-activated autophagy enhanced bacterial killing and major histocompatibility complex class II-dependent antigen presentation in primary human dendritic cells and that this process was dependent on *ATG16L1*, Nod2, and the signaling adaptor RICK but not NLRP3.³⁰ Another group showed that Nod1 and Nod2 stimulate autophagy in a RICK- and NF- κ B-independent manner, possibly through *ATG16L1* recruitment bacterial entry sites.³¹ Our findings confirm these results and clarify discrepancies between these reports, supporting a role for Nod2-dependent signaling mediated by RICK but not NF- κ B in this process.

Autophagy is also implicated in the delivery of microbial ligands to intracellular compartments containing TLRs to stimulate an antimicrobial response. Autophagy is essential for the stimulation of TLR7 and TLR8 by viral single-stranded RNA^{25,32} as well as the delivery of costimulatory ligands to TLR9.³³ Our results implicate autophagy in intracellular trafficking of MDP essential for Nod2-dependent signaling. However, it should be noted that autophagy inhibition did not completely ablate MDP-stimulated Nod2 signaling, suggesting a redundant mechanism in this process. This agrees with reports showing multiple entry routes for MDP into cells, as well as cell type-specific mechanisms for uptake.⁴ For example, a recent study shows no difference in MDP-stimulated cytokine secretion between wild-type or *ATG16L1* null mouse macrophages,²⁹ whereas our data in human epithelial cell lines show a dramatic reduction in MDP-stimulated NF- κ B activity when *ATG16L1* expression is knocked down. Our results suggest autophagy is an additional, novel mechanism for MDP intracellular trafficking that may contribute to a positive feedback loop during intracellular bacterial infection.

The *ATG16L1* T300A risk variant is highly prevalent in healthy individuals (0.53).⁷ In our study of cells from healthy donors, the *ATG16L1* T300A variant specifically

impaired Nod2-dependent antibacterial function in colon epithelial cells but not in monocytic cells. This is in contrast to recent reports showing MDP-stimulated autophagy impairment in dendritic cells and lymphoblastoid cells from patients with CD with the *ATG16L1* T300A variant.^{30,31} This raises the intriguing possibility of other pathway modulators (environmental, microbial, genetic, and so on) contributing to pathway impairment and disease development. In addition, severe Paneth cell abnormalities were found in patients with CD carrying the *ATG16L1* T300A variant³⁴ or *NOD2* risk variants.³⁵ In mice, Nod2 deficiency results in increased intestinal bacterial load and greater susceptibility to pathogenic bacterial colonization.³⁶ This finding could result from Paneth cell dysfunction, defects in intestinal autophagic responses, or more likely a combination of the two. Our results suggest that in addition to Paneth cell defects, *ATG16L1* and *NOD2* risk variants alter intestinal epithelial cell antimicrobial responses, potentially altering the amount or composition of gut bacteria and increasing CD susceptibility.

Finally, we showed that both *ATG16L1* and *NOD2* contribute to an autophagy-dependent antibacterial pathway that is altered in a cell type-specific manner by CD-associated mutations. Two additional CD risk genes (*IRGM* and *NCF4*) have obvious links to autophagy, making them candidates for inclusion in this pathway as well.³⁷ Future studies will need to examine the contribution of these and other CD risk genes to this autophagic, antimicrobial pathway. Examining the interplay of risk genes may lead to additional, more effective, and individually tailored treatments for CD based on underlying disease mechanisms.

Supplementary Material

Note: To access the supplementary material accompanying this article, visit the online version of *Gastroenterology* at www.gastrojournal.org, and at doi: 10.1053/j.gastro.2010.07.006.

References

- Baumgart DC, Carding SR. Inflammatory bowel disease: cause and immunobiology. *Lancet* 2007;369:1627–1640.
- Rutgeerts P, Goboos K, Peeters M, et al. Effect of faecal stream diversion on recurrence of Crohn's disease in the neoterminal ileum. *Lancet* 1991;338:771–774.
- Sartor RB. Therapeutic manipulation of the enteric microflora in inflammatory bowel diseases: antibiotics, probiotics, and prebiotics. *Gastroenterology* 2004;126:1620–1633.
- Inohara N, Chamailard M, McDonald C, et al. NOD-LRR proteins: role in microbial-host interactions and inflammatory disease. *Ann Rev Biochem* 2005;74:355–383.
- Abraham C, Cho JH. Functional consequences of NOD2 (CARD15) mutations. *Inflamm Bowel Dis* 2006;12:641–650.
- Wellcome Trust Case Control Consortium. Genome-wide association study of 14,000 cases of seven common diseases and 3,000 shared controls. *Nature* 2007;447:661–678.
- Hampe J, Franke A, Rosenstiel P, et al. A genome-wide association scan of nonsynonymous SNPs identifies a susceptibility variant for Crohn disease in *ATG16L1*. *Nat Genet* 2007;39:207–211.
- Massey DC, Parkes M. Common pathways in inflammatory diseases revealed by genomics. *Gut* 2007;56:1489–1492.
- Rioux JD, Xavier RJ, Taylor KD, et al. Genome-wide association study identifies new susceptibility loci for Crohn disease and implicates autophagy in disease pathogenesis. *Nat Genet* 2007;39:596–604.
- Schmid D, Munz C. Innate and adaptive immunity through autophagy. *Immunity* 2007;27:11–21.
- Pineton de Chambrun G, Colombel JF, et al. Pathogenic agents in inflammatory bowel diseases. *Curr Opin Gastroenterol* 2008;24:440–447.
- Kuballa P, Huett A, Rioux JD, et al. Impaired autophagy of an intracellular pathogen induced by a Crohn's disease associated *ATG16L1* variant. *PLoS One* 2008;3:e3391.
- McDonald C, Chen FF, Ollendorff V, et al. A role for Erbin in the regulation of Nod2-dependent NF-kappaB signaling. *J Biol Chem* 2005;280:40301–40309.
- Franchi L, Amer A, Body-Malapel M, et al. Cytosolic flagellin requires IpaF for activation of caspase-1 and interleukin 1beta in salmonella-infected macrophages. *Nat Immunol* 2006;7:576–582.
- Debnath J. Detachment-induced autophagy in three-dimensional epithelial cell cultures. *Methods Enzymol* 2009;452:423–439.
- Birmingham CL, Brumell JH. Autophagy recognizes intracellular Salmonella enterica serovar Typhimurium in damaged vacuoles. *Autophagy* 2006;2:156–158.
- Marina-Garcia N, Franchi L, Kim YG, et al. Pannexin-1-mediated intracellular delivery of muramyl dipeptide induces caspase-1 activation via Cryopyrin/NLRP3 independently of Nod2. *J Immunol* 2008;180:4050–4057.
- Martinon F, Agostini L, Meylan E, et al. Identification of bacterial muramyl dipeptide as activator of the NALP3/cryopyrin inflammasome. *Curr Biol* 2004;14:1929–1934.
- Inohara N, Ogura Y, Fontalba A, et al. Host recognition of bacterial muramyl dipeptide mediated through NOD2. *J Biol Chem* 2003;278:5509–5512.
- Mizushima N, Yoshimori T, Levine B. Methods in mammalian autophagy research. *Cell* 2010;140:313–326.
- Criollo A, Senovilla L, Authier H, et al. The IKK complex contributes to the induction of autophagy. *EMBO J* 2010;29:619–631.
- Marina-Garcia N, Franchi L, Kim YG, et al. Clathrin- and dynamin-dependent endocytic pathway regulates muramyl dipeptide internalization and NOD2 activation. *J Immunol* 2009;182:4321–4327.
- Herskovits AA, Auerbuch V, Portnoy DA. Bacterial ligands generated in a phagosome are targets of the cytosolic innate immune system. *PLoS Pathog* 2007;3:e51.
- Lapaquette P, Glasser AL, Huett A, et al. Crohn's disease-associated adherent-invasive *E. coli* are selectively favoured by impaired autophagy to replicate intracellularly. *Cell Microbiol* 2010;12:99–113.
- Delgado MA, Elmaoued RA, Davis AS, et al. Toll-like receptors control autophagy. *EMBO J* 2008;27:1110–1121.
- Sanjuan MA, Dillon CP, Tait SW, et al. Toll-like receptor signalling in macrophages links the autophagy pathway to phagocytosis. *Nature* 2007;450:1253–1257.
- Shi CS, Kehrl JH. MyD88 and Trif target Beclin 1 to trigger autophagy in macrophages. *J Biol Chem* 2008;283:33175–33182.
- Xu Y, Jagannath C, Liu XD, et al. Toll-like receptor 4 is a sensor for autophagy associated with innate immunity. *Immunity* 2007;27:135–144.

29. Saitoh T, Fujita N, Jang MH, et al. Loss of the autophagy protein Atg16L1 enhances endotoxin-induced IL-1 β production. *Nature* 2008;456:264–268.
30. Cooney R, Baker J, Brain O, et al. NOD2 stimulation induces autophagy in dendritic cells influencing bacterial handling and antigen presentation. *Nat Med* 2010;16:90–97.
31. Travassos LH, Carneiro LA, Ramjeet M, et al. Nod1 and Nod2 direct autophagy by recruiting ATG16L1 to the plasma membrane at the site of bacterial entry. *Nat Immunol* 2010;11:55–62.
32. Lee HK, Lund JM, Ramanathan B, et al. Autophagy-dependent viral recognition by plasmacytoid dendritic cells. *Science* 2007;315:1398–1401.
33. Chaturvedi A, Dorward D, Pierce SK. The B cell receptor governs the subcellular location of Toll-like receptor 9 leading to hyperresponses to DNA-containing antigens. *Immunity* 2008;28:799–809.
34. Cadwell K, Liu JY, Brown SL, et al. A key role for autophagy and the autophagy gene Atg16L1 in mouse and human intestinal Paneth cells. *Nature* 2008;456:259–263.
35. Wehkamp J, Harder J, Weichenthal M, et al. NOD2 (CARD15) mutations in Crohn's disease are associated with diminished mucosal alpha-defensin expression. *Gut* 2004;53:1658–1664.
36. Petnicki-Ocwieja T, Hrcir T, Liu YJ, et al. Nod2 is required for the regulation of commensal microbiota in the intestine. *Proc Natl Acad Sci U S A* 2009;106:15813–15818.
37. Roberts RL, Hollis-Moffatt JE, Geary RB, et al. Confirmation of association of IRGM and NCF4 with ileal Crohn's disease in a population-based cohort. *Genes Immun* 2008;9:561–565.

Received November 6, 2009. Accepted July 7, 2010.

Reprint requests

Address requests for reprints to: Christine McDonald, PhD, Department of Pathobiology, NC22, Lerner Research Institute, Cleveland Clinic, 9500 Euclid Avenue, Cleveland, Ohio 44195. e-mail: mcdonac2@ccf.org; fax: (216) 636-0104.

Acknowledgments

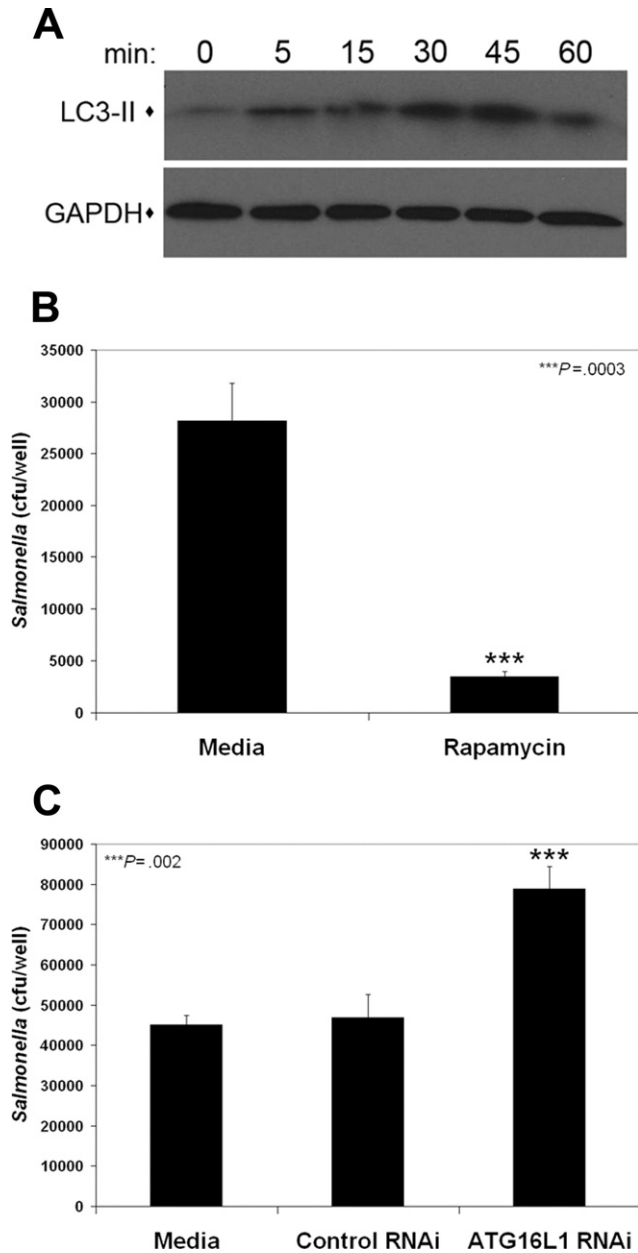
The authors thank all the members of the Cleveland Clinic's Inflammatory Bowel Disease group; Laura Nagy and Derek Abbott for their constructive comments; Judy Drazba and Amit Vasanji for their imaging assistance; James Bena for help with statistical analysis; Keyonna Smith for recruiting subjects for this study; all the individuals who donated blood; Brian Rubin, Gabriel Nuñez, Gerhard Rogler, Derek Abbott, Tony Eissa, and William Maltese for reagents; and Luigi Franchi for advice on *Salmonella* infection assays.

Conflicts of interest

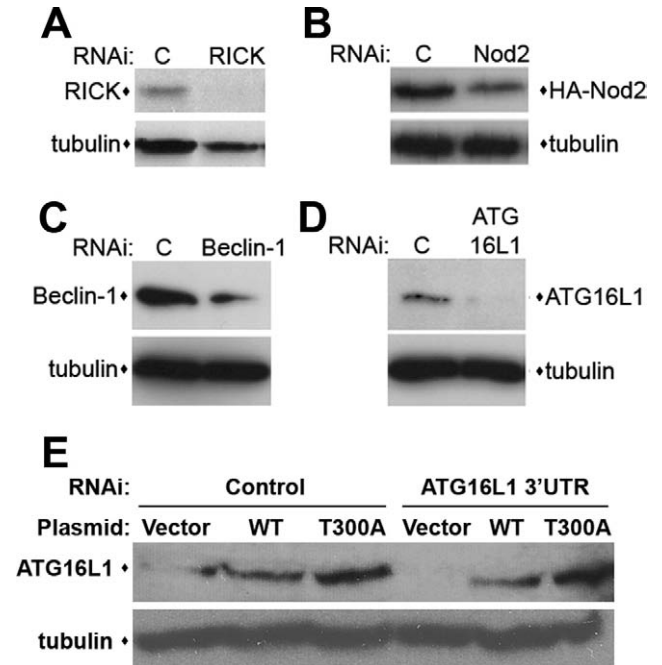
The authors disclose no conflicts.

Funding

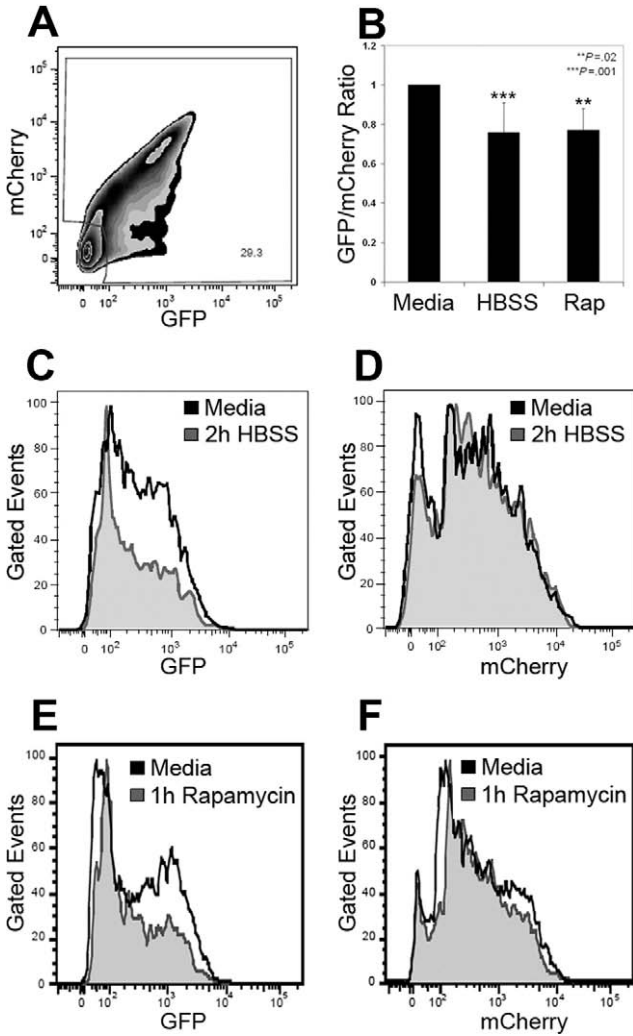
Supported by a Career Development Award from the Crohn's & Colitis Foundation of America (to C.M.), National Institutes of Health research grants R01DK082437 (to C.M.) and K23DK068112 (to J.-P.A.), and in part by the generosity of Gerald and Nancy Goldberg, Kenneth and Jennifer Rainin, and the National Institutes of Health National Center for Research Resources, CTSA 1UL1RR024989 (Cleveland, OH).



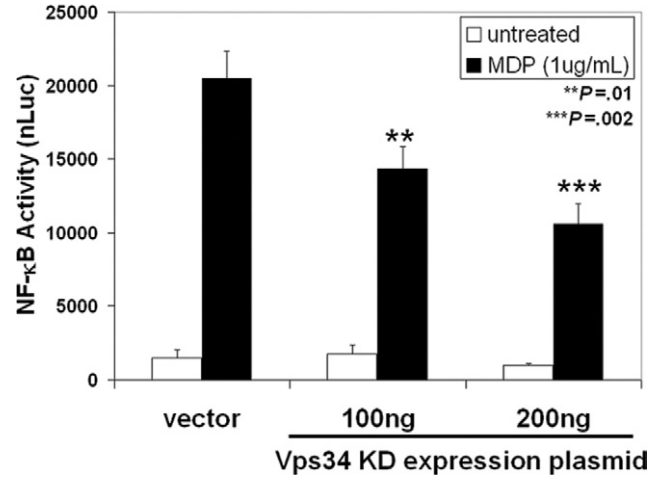
Supplementary Figure 1. *Salmonella* is killed via autophagy. (A) Immunoblot analysis of HCT116 cells infected with *Salmonella* for the indicated times. (B) Gentamicin protection assay performed in *Salmonella*-infected HCT116 cells treated with rapamycin (25 μ g/mL) (mean \pm SD). (C) Gentamicin protection assay performed in *Salmonella*-infected HCT116 cells transfected with control or ATG16L1 RNAi (mean \pm SD).



Supplementary Figure 2. Immunoblots showing efficiency of RNAi knockdown of indicated gene 48 hours after transfection in the following cells: (A) HEK293T, (B) HEK293T transfected with HA-Nod2, and (C and D) HCT116. (E) HT29GR cells transfected with control or ATG16L1 3' untranslated region RNAi and the indicated ATG16L1 complementary DNA expression constructs.



Supplementary Figure 3. Flow cytometric analysis of HEK293T cells transfected with GFP-mCherry-LC3. (A) GFP versus mCherry density plot showing the gated population used for analysis of relative MFI. (B) Quantification of the change in GFP/mCherry ratio in response to Hank's balanced salt solution starvation for 2 hours or rapamycin treatment (25 $\mu\text{g}/\text{mL}$, Rap) for 1 hour relative to cells maintained in media (mean \pm SD; media, n = 10; Hank's balanced salt solution, n = 9; Rap, n = 5). (C) Representative histogram of GFP MFI of the mCherry-positive population of cells maintained in media or starved in Hank's balanced salt solution for 2 hours. (D) Representative histogram of mCherry MFI of the mCherry-positive population of cells maintained in media or starved in Hank's balanced salt solution for 2 hours. (E) Representative histogram of GFP MFI of the mCherry-positive population of cells maintained in media or treated with rapamycin (25 $\mu\text{g}/\text{mL}$) for 1 hour. (F) Representative histogram of mCherry MFI of the mCherry-positive population of cells maintained in media or treated with rapamycin (25 $\mu\text{g}/\text{mL}$) for 1 hour.



Supplementary Figure 4. NF- κ B luciferase reporter assay performed in HCT116 cells transfected with the indicated amounts of kinase-dead Vps34 (Vps34 KD) expression plasmid. Cells treated with media or MDP (1 $\mu\text{g}/\text{mL}$) for 16 hours. Luciferase values normalized to β -gal transfection control (nLuc) (mean \pm SD).